Dynamically isotropic Gough-Stewart Platform design with flexural joints

Yogesh Pratap Singh[1*], Nazeer Ahmad[2] and Ashitava Ghosal[1*]

[1*]Department of Mechanical Engineering, Indian Institute of Science, Bangalore, 560012, India.
[2]URSC, Indian Space Research Organization, Bangalore, 560017, India.

*Corresponding author(s). E-mail(s): yogeshsingh@iisc.ac.in; asitava@iisc.ac.in ;
Contributing authors: nazeer@ursc.gov.in;

Abstract

A dynamically isotropic Modified Gough-Stewart platform (MGSP), with equal first six natural frequencies, is well-suited for micro-vibration isolation as it allows for the utilization of identical dampers resulting in effective vibration isolation. In an earlier work, a novel geometry-based approach was developed to deduce the design parameters of a dynamically isotropic MGSP with conventional kinematic joints. In spacecraft applications, kinematic joints may introduce friction, backlash errors, and lubrication-related issues can negatively impact the vibration isolation characteristics of the MGSP. In this work, an MGSP with flexural joints is considered and different designs are evaluated by considering their dynamic isotropic index (DII), manufacturing feasibility, and static and dynamic characteristics. The DII is a critical metric, representing the ratio of the largest to the smallest natural frequency among the first six modes, quantifying the frequency spread. Simulations of the developed designs were performed in a finite element analysis software ANSYS. A prototype of the MGSP with flexural joints was built, and experiments were conducted to extract the frequencies associated with the $\boldsymbol{X}$, $\boldsymbol{Y}$, and $\boldsymbol{Z}$ modes. The natural frequencies obtained through simulation range from 43 to 45 Hz and matched very closelly with the experiemental results. Additionally, a damping of 6-7 % across all modes was achieved. The agreement between the analytical, simulation, and experimental results validates our design approach and demonstrates its suitability for micro-vibration isolation applications in spacecraft.

Keywords: Dynamic isotropy, Modified Gough-Stewart Platform, Flexural Joint, Damping

1 Introduction

Rotating, reciprocating components and spacecraft operations often generate micro-vibrations with frequencies of up to 250 Hz [1]. These micro-vibrations have a detrimental impact on the performance of optical payloads installed on the spacecraft's structure. The implementation of a six Degree of Freedom (DOF) Gough-Stewart platform (GSP) is suggested in the literature to isolate these micro-vibrations from the sensitive payloads [2–5]. To achieve effective vibration isolation, the equivalence of the first six natural frequencies for translation and rotation is an ideal design [2, 6, 7]. To achieve this optimal condition, the use of a dynamically isotropic GSP with first six natural frequencies being equal has been advocated. A Modified GSP (MGSP) is suggested in this work since conventional GSP designs fail to achieve the dynamic isotropy [8–10]. In an MGSP, the connection points are distributed along two radii on both platforms (as shown in Fig. 1a), as opposed to the single radius arrangement in conventional GSPs. In dynamically isotropic MGSP configurations, tuning dampers for passive vibration isolation becomes straightforward, as identical dampers can be employed across the given frequency bandwidth. Additionally, achieving dynamic isotropy simplifies active vibration control, as it enables the use of a decoupled control strategy – a multi-input-multi-output (MIMO) GSP is converted into six single-input-single-output (SISO) systems, streamlining the control process [11].

In a design that lacks isotropy, the isolation region for a specific DOF (for example, mode $\boldsymbol{X}$ as shown in Fig. 1b) can be negatively influenced by the presence of peaks of cross-DOFs (such as Rot($\boldsymbol{X}$) in Fig. 1b) overlapping over it. To achieve a well-defined isolation region (after $\sqrt{2}\omega$) without interference from other modes, a design of an MGSP should ideally consolidate all the peaks ideally in a single location. Previous research has attempted to provide closed-form solutions for dynamic isotropy [8–10], but the procedure to obtain the design parameters are coupled and complex, making the design process challenging or confined to some specific symmetrical configuration [12]. Our prior work introduced an innovative geometry-based approach that simplifies the MGSP dynamic isotropy problem in three-dimensional space into a two-dimensional geometry problem [6]. It was shown that all the design variables for an MGSP exhibited certain relationships through a pair of triangles. This approach allowed us to derive general analytical closed-form solutions for the design variables in explicit forms, making the design process significantly more streamlined and straightforward along with ensuring practical feasibility.

In the context of spacecraft applications, the use of conventional joints, such as spherical or universal joints, introduces issues related to friction, backlash errors, and lubrication [3, 5, 11]. These issues can potentially disrupt the vibration isolation characteristics of the MGSP. To address these challenges, conventional joints are substituted with flexural hinges, albeit with the trade-off of introducing some additional parasitic stiffness. While some researchers, including Hanieh in [5], Preumont et al. in [3], and others, have proposed designs incorporating flexural joints into conventional cubic GSPs, and Yun et al. in [11] suggested the integration of flexural joints in a specific variant of the MGSP for telescope secondary mirrors, none of the papers have provided comprehensive insights into the development of an MGSP with flexural joints to the best of our knowledge. This paper fills this knowledge gap by first

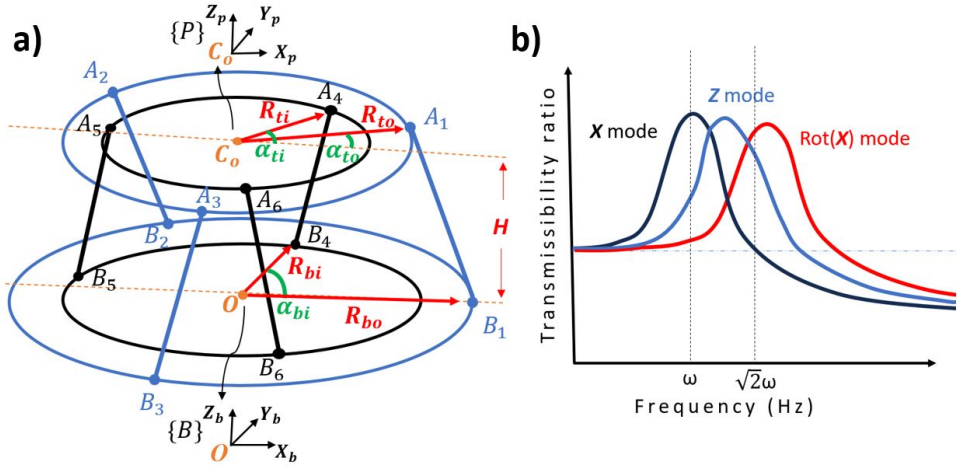

Fig. 1 a) Two-radii or Modified Gough-Stewart platform b) Transmissibility curve in a non isotropic design.

discussing a geometry-based approach to achieving a dynamically isotropic design for an MGSP. Subsequently, the design is extended to incorporate flexural joints, relaxing certain analytical assumptions. Finally, experimental results from a prototype of the MGSP featuring flexural joints are presented. Close agreement observed among analytical, simulation, and experimental results validates the approach of this work.

2 Analytical formulation

A Modified Gough-Stewart Platform (MGSP) consists of a mobile top platform, a fixed base platform, and six actuated legs in between them. The payload (micro-vibration-inducing element) will be mounted on the top platform for spacecraft applications with passive damping. The fixed base will be mounted on the spacecraft bus, and the six legs will provide the necessary damping/stiffness. The legs are conventionally connected to the mobile platform through a spherical joint and to the bottom platform through a spherical or an universal joint. The mechanism thus provide 6-DOF high-precision pointing and positioning.

With reference to Fig. 1a, the coordinates of a point on the base frame $\{B\}$ are denoted by $\{x_b, y_b, z_b\}$ and on the top or moving frame $\{P\}$ by $\{x_p, y_p, z_p\}$. In an MGSP, the connecting points are placed at two radii on each platform, as shown in Fig. 1a. The variables R_{bo} and R_{bi} denote the outer and inner radii of the bottom platform, while the variables R_{to} and R_{ti} denote the outer and inner radii of the top platform. There are two sets of three legs with identical lengths, and each leg in a set is uniformly spaced from each other by an angular spacing of 120° angle along the circumference. The vector $\boldsymbol{OB_1}$ (magnitude equal to R_{bo}) is chosen along $\boldsymbol{X_b}$ direction. The vectors $\boldsymbol{C_oA_1}$, $\boldsymbol{OB_4}$, and $\boldsymbol{C_oA_4}$ makes an angle α_{to}, α_{bi}, α_{ti} with $\boldsymbol{X_b}$. The variable H denotes the vertical distance between centers of the two platforms at the neutral position.

Each leg is assumed to have an axial stiffness of k in its joint space. The stiffness matrix $[\mathbf{K}_T]$ in the task space [5, 6] is given by:

$$[\mathbf{K}_T] = k[\mathbf{B}][\mathbf{B}]^T \tag{1}$$

The force transformation matrix ($[\mathbf{B}]$) is a transpose of an inverse Jacobian ($[\mathbf{J}]$) and is given by $[\mathbf{B}]=([\mathbf{J}^{-1}])^T$ where $[\mathbf{B}]$ is given by:

$$[\mathbf{B}]_{6\times 6} = \begin{bmatrix} \boldsymbol{s_1} & \dots & \boldsymbol{s_6} \\ ({}^B[\mathbf{R}]_P({}^P\boldsymbol{p_1})) \times \boldsymbol{s_1} & \dots & ({}^B[\mathbf{R}]_P({}^P\boldsymbol{p_6})) \times \boldsymbol{s_6} \end{bmatrix} \tag{2}$$

with $\boldsymbol{s_j} = \dfrac{{}^B\boldsymbol{t} + {}^B[\mathbf{R}]_P\, {}^P\boldsymbol{p_j} - {}^B\boldsymbol{b_j}}{l_j}$, $j = 1, \dots, 6$.

The vector $\boldsymbol{s}_j$ is a unit vector along the leg j and the variable l_j is the length of the respective leg. The vector ${}^B\boldsymbol{t}$ connects the centers of two platforms, ${}^P\boldsymbol{p_j}$ is the location of the connection points on the top platform with respect to the moving frame $\{P\}$, and ${}^B\boldsymbol{b_j}$ is the location of the connection points at the base with respect to the fixed frame $\{B\}$. The rotation matrix ${}^B[\mathbf{R}]_P$ represents the orientation of the mobile platform with respect to the fixed base. If the orientation of the payload's principal axes is chosen to be coincident with the coordinate system, then the diagonal structure of the mass matrix $[\mathbf{M}]$ can be obtained as:

$$[\mathbf{M}] = \text{diag}[\, m_p,\ m_p,\ m_p,\ I_{xx},\ I_{yy},\ I_{zz}] \tag{3}$$

where m_p represents the mass of the payload (including the mobile platform) and I_{xx}, I_{yy}, and I_{zz} represents its moment of inertia along each direction with respect to its center of mass (COM). From Eqs. (1), (2) and (3), the natural frequency matrix $[\mathbf{G}]$ in the task space [6, 8–10] can be obtained as:

$$[\mathbf{G}]_{6\times 6} = [\mathbf{M}]^{-1}[\mathbf{K_T}] = [\mathbf{M}]^{-1}k[\mathbf{B}][\mathbf{B}]^T \tag{4}$$

The natural frequency matrix $[\mathbf{G}]$ will be function of the design variables of an MGSP, i.e., R_{bo}, R_{to}, R_{bi}, R_{ti}, H, a, α_{to}, and $(\alpha_{bi} - \alpha_{ti})$, where a is the leg length ratio $a = l_{o2}/l_{o1}$ (Note $l_{o1} = l_1 = l_2 = l_3$ and $l_{o2} = l_4 = l_5 = l_6$). For dynamic isotropy, all the six eigenvalues of the natural frequency matrix $[\mathbf{G}]$ must be equal and we can write

$$\lambda_1 = \lambda_2 = \lambda_3 = \lambda_4 = \lambda_5 = \lambda_6 = \omega^2 \tag{5}$$

where, ω is the natural frequency of the MGSP and λ_1 to λ_6 are the six eigenvalues of the matrix $[\mathbf{G}]$. Designing MGSP in its neutral position is a practically feasible approach in an application requiring precise control and a small workspace such as vibration isolation. At this neutral position, the two platforms are parallel to each other with their centres on the same vertical line (${}^B[\mathbf{R}]_P = [\mathbf{I}]$ and ${}^B\boldsymbol{t} = [\ 0\ 0\ H\ ]^T$). The MGSP operating around its neutral position offers the advantage of obtaining closed-form solutions for dynamic isotropy due to its geometrical symmetries.

Using the methodology described above for obtaining dynamic isotropy conditions, the analytical closed-form solution for all the design variables was obtained in explicit form in our previous work [6, 7]. The solution for a 3-dimensional dynamically isotropic

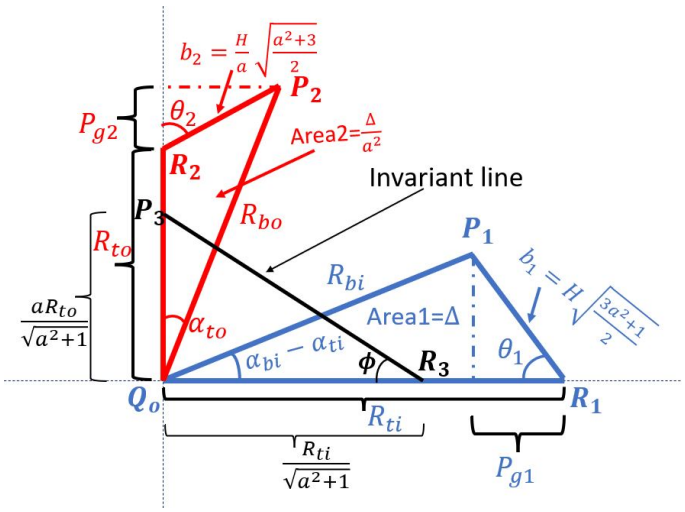

Fig. 2 Geometrical interpretation of design variables of an MGSP [6]

MGSP was obtained using a 2D geometry-based approach. The observations made by simplifying the obtained transcendental equation led to a geometric-based approach where the design variables were seen to be related by a pair of triangles, as shown in Fig. 2. Each triangle pair with a certain geometrical relationship represents a dynamically isotropic configuration, and all the design variables can be deduced by finding the sides of any triangle pair. Since the dynamic isotropy problem of an MGSP has multiple solutions, the selection of a particular triangle pair (or, in turn, design variables) depends on space and the loading constraints for the application it is to be designed for. The in-depth development of the mentioned geometry-based approach is available in references [6, 7].

Simulations were performed in ANSYS with the dynamically isotropic design of an MGSP obtained using the geometry-based approach, and the first six natural frequencies were found very close to each other in each case (i.e., all $\omega = \sqrt{\frac{2k}{m_p}}$). These simulations had similar assumptions as in the analytical formulation, i.e., the legs have ideally zero mass and only the axial stiffness k while the platform has a high stiffness to push the modes of the platforms to very high frequencies above the required isolation region.

3 MGSP Design

A conventional joint (spherical or universal) can introduce friction, backless error, and lubrication-related issues that can alter the vibration isolation characteristics of the MGSP in spacecraft applications. To overcome this, the conventional joints are replaced by flexural hinges at the expense of some additional parasitic stiffness. An ideal flexural joint for this application should have high axial stiffness, high shear stiffness, low bending and torsional stiffness [3, 5, 11]. Each leg must have high axial stiffness to bear the distributed launch loads. In the case of active vibration isolation,

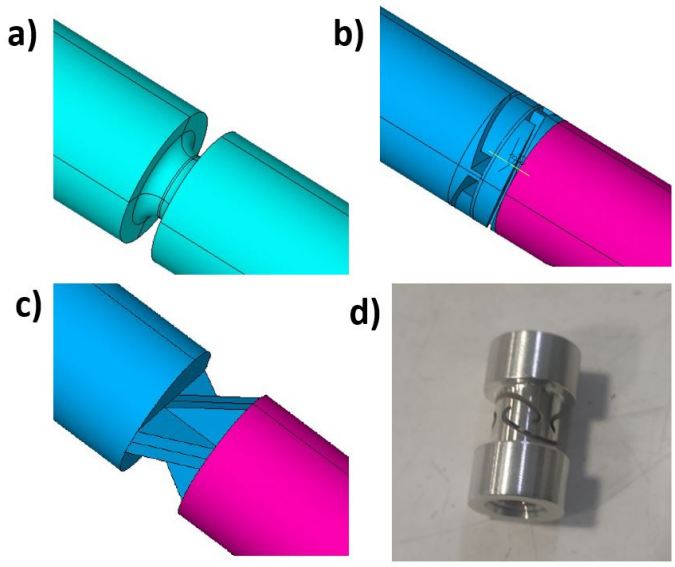

Fig. 3 Various flexural joints investigated

a high axial stiffness is required to pass the control loads to the mobile platform. Similarly, high shear stiffness of the joints will push the local modes of the legs to a higher frequency, preventing its interference in the region of isolation of MGSP in our application. Low bending and torsional stiffness ensure that the spread of six natural frequencies confines to a very narrow bandwidth. In the case of active control, the rotary stiffness of the flexural joint determines the zeros of the system. The dimensions of the flexural joint are capped by load-bearing capacity (static) and displacement characteristics required for any application. The contribution of small bending stiffness $[\mathbf{K}_b]$ in the analytical model [5] would practically modify the overall stiffness matrix in Eqn (1) as:

$$[\mathbf{K}_T] = k[\mathbf{B}][\mathbf{B}]^T + [\mathbf{K}_b] \tag{6}$$

However, the effect of the $[\mathbf{K}_b]$ term is small and is generally not considered for analytical-based design. Considering the above design philosophy for a flexural joint, various flexural joints were investigated, as shown in Fig. 3. The selection of a flexural joint is based on the dynamic isotropic index (DII), manufacturing feasibility, and its static and dynamic characteristics. As already discussed, that complete isotropy condition in the original analytical model will now be perturbed due to various types of stiffness in a flexural hinge. A DII parameter is used to quantify the natural frequencies spread around the dynamically isotropic natural frequency $\sqrt{2k/m_p}$ – DII is the ratio of the largest to the smallest natural frequency among the first six modes and is expected to be as close to one or ideally one.

A finite element (FE) model of the MGSP with flexural joints, as shown in Fig. 4, has the following components:

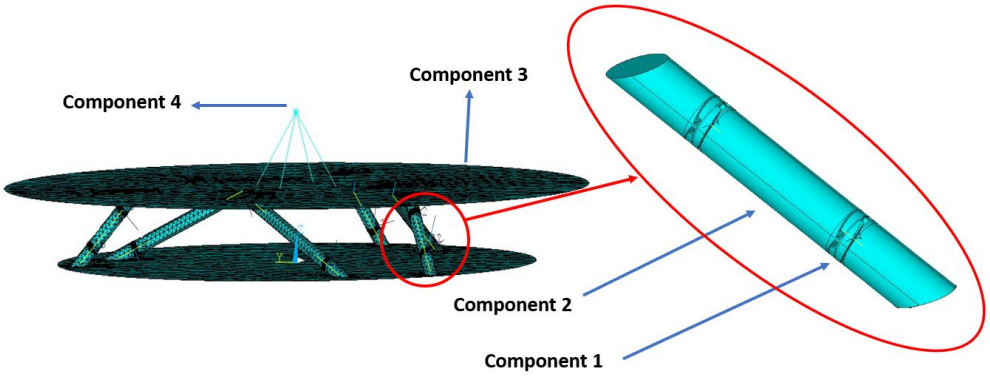

Fig. 4 FE model of MGSP based on one of the flexural joints

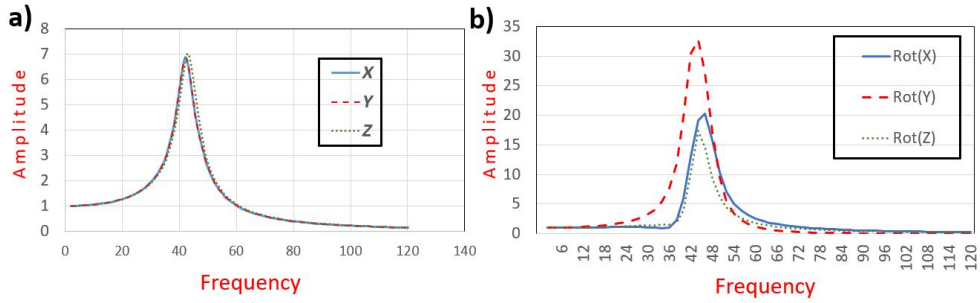

Fig. 5 a) Simulation results for $\boldsymbol{X}, \boldsymbol{Y}$, and $\boldsymbol{Z}$ DOFs b) Simulation results for rotational $\boldsymbol{X}, \boldsymbol{Y}$, and $\boldsymbol{Z}$ DOFs

- All the flexural joints (shown as Component 1 in Fig. 4) explored are made of Aluminium alloy. This relaxes some of our assumptions during formulation that the legs are massless with only axial stiffness. A small value of mass (as compared to payloads') and bending stiffness will slightly increase the value of DII ≈ 1, but the effect is expected to be small.
- Component 2 in Fig. 4 made of the Aluminium alloy provides the necessary stiffness after the static analysis under the launch load conditions. As per the analytical model, two sets of legs have different lengths but must have an equal axial stiffness. The following can be done by adjusting the cross-section area according to EA/l .
- Component 3, i.e., the mobile platform, is designed for very high stiffness to push the plate's local mode to higher values.
- The payload mass/inertia is shown as lumped mass (see Component 4).

All the legs (treated as continuous metal structures with flexural joints) are given an equivalent viscous damping $\zeta = 3.5$ % (within standard range) pertaining to their inherent material/hysterics damping properties. The introduction of damping will not affect the resonance frequencies, and our analytical result for dynamic isotropic natural frequencies remains intact.

Table 1 Comparison of natural frequencies for MGSP obtained via analytical solution, Simulation, and Experiment in hertz

Modes	$\boldsymbol{X}$	$\boldsymbol{Y}$	$\boldsymbol{Z}$	Rot $\boldsymbol{X}$	Rot $\boldsymbol{Y}$	Rot $\boldsymbol{Z}$
Analytical	43.3	43.3	43.3	43.3	43.3	43.3
Simulation	43	43	43	45.5	43.5	44.5
Experiment	43	43	45	-	-	-

Table 2 Comparison of damping for MGSP obtained via Simulation and Experiment

Damping %	$\boldsymbol{X}$	$\boldsymbol{Y}$	$\boldsymbol{Z}$	Rot $\boldsymbol{X}$	Rot $\boldsymbol{Y}$	Rot $\boldsymbol{Z}$
Simulation	7.50	7.44	7.44	6.50	7.38	5.00
Experiment	7.80	7.80	5.30	-	-	-

4 Results and observations

A typical spacecraft wheel with mass properties $m_p = 5$ Kg, $I_{xx} = 2.5448921166 \times 10^{-2}$ Kg m^2, $I_{yy} = 2.5448921166 \times 10^{-2}$ Kg m^2, and $I_{zz} = 4.3068973334 \times 10^{-2}$ Kg m^2 is used. The simulation using the dynamically isotropic configuration gave a DII = 1.09 for Flexural 1 (See Fig. 3a), DII = 1.13 for flexural 2 (See Fig. 3b), and DII=1.15 (See Fig. 3c) for flexural 3. An equivalent stiffness of $1.85 - 2.0 \times 10^5$ N/m for each leg is maintained in each case. After studying the manufacturing feasibility, the flexural joint, as shown in Fig. 3d, is being used, which can be realized through electrical discharge machining. The amplitude vs. frequency curves obtained from the simulation for $\boldsymbol{X}, \boldsymbol{Y}$, and $\boldsymbol{Z}$ DOFs are shown in the Fig. 5a. A unit displacement/rotation was given to the base plate's nodes, and the response was noted at the lumped mass. It can be observed that all three curves for translational modes overlap each other with a natural frequency of around 43 Hertz. A similar result is obtained analytically using dynamically isotropic natural frequency (i.e., $\sqrt{2k/m_p} = 43.3$ Hertz). This validates our simulation and analytical results for dynamically isotropic MGSP, as shown in Table 1. A slight deviation of 0.3 hertz is expected due to a step size of 0.5 hertz taken for computational purposes. The overall structural damping obtained using the half-power bandwidth method for the MGSP has the same damping in all three directions, as summarized in Table 2 ($\zeta \approx 7.5\%$). This also implies that the dynamically isotropic configuration equally distributes the damping. A similar observation can be seen in Fig. 5b for rotational modes as well and is summarized in Table 1.

A prototype of MGSP with flexural joints is built along similar lines and the first three modes were captured in the initial experimentation at the ISRO test facility. The lateral modal survey test ($\boldsymbol{X}$and $\boldsymbol{Y}$) was done by mounting the fixed base on the slip table and the longitudinal ($\boldsymbol{Z}$ axis) test was done on mounting the base to a 4-ton electrodynamic shaker, as shown in Fig. 6. The base platform was excited with an acceleration sine sweep of the constant amplitude of 0.5 g sweeping from 10-500 Hz. The response was measured using tri-axial accelerometers (make: B & K model). The resonance peaks obtained for $\boldsymbol{X}, \boldsymbol{Y}$, and $\boldsymbol{Z}$ DOFs are 43, 43, and 45 Hz, respectively, further verifying our analytical and simulation results. The slight deviation of resonance peak 1 Hz is due to the difference in stiffness of the legs from the intended

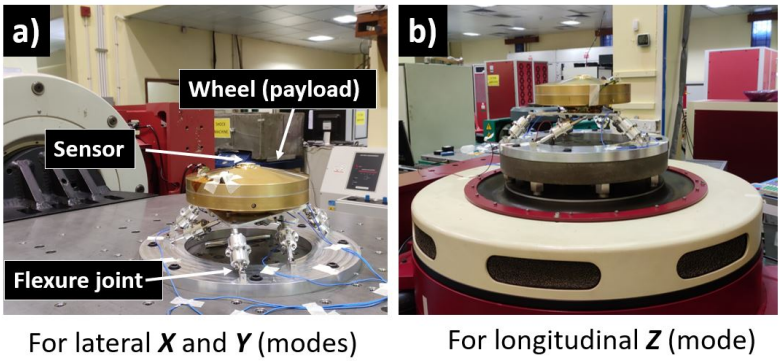

Fig. 6 MGSP Prototype based on flexural joints with experimental setup

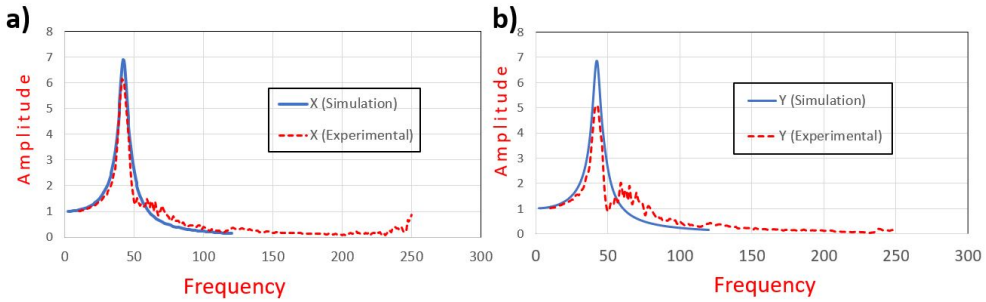

Fig. 7 Amplitude vs. frequency curve for $\boldsymbol{X}$ and $\boldsymbol{Y}$ modes obtained using simulation and experimentation

value due to a slight variation in the actual material properties. Figure 7 shows a close resemblance of the Amplitude vs. frequency curve for $\boldsymbol{X}$ and $\boldsymbol{Y}$ modes obtained using simulation and experimentation. The analytical, simulation, and experimental results are summarized in Table 1 and 2, validating our design for the micro-vibration isolation application where all six natural frequencies are nearly the same. It is to be noted that a structural damping system has a better isolator performance in the isolation region than a viscous damper with the same amplification/resonance peak.

5 Discussion and future work.

The results obtained with the current design are encouraging for our application, but a discussion on scopes of improvements from the authors' observation may be insightful for future explorations. The initial simulation results with flexural joints made of Ti alloys (instead of Al alloys) offer better DII, however, at the expense of cost associated with the titanium. Another way to reduce DII and, hence, the frequency bandwidth is by adjusting the offset of the flexural joint. As shown in Fig. 8, the calculated anchoring points (conventional joints in analytical formulation) are A_1 and B_1; however, the position of the flexural bending point is slightly adjusted to $A_1{}'$ and $B_1{}'$ points, respectively, to avoid interference of leg with the platform during operation.

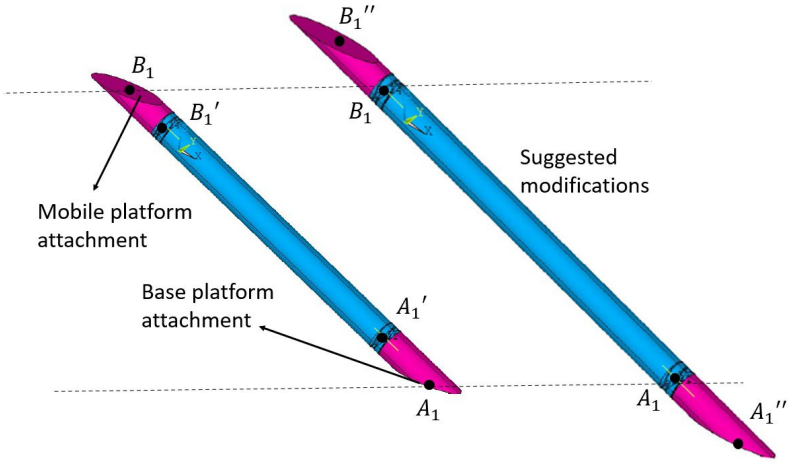

Fig. 8 Adjustment of attachment points suggested to improve DII

To modify the flexural joint bending point to A_1 and B_1 and resemble the analytical model with even higher precision, we must design the MGSP for A_1'' and B_1'' as the platform attachment point lying along the same line and extended beyond $A_1 - B_1$ such that flexural joints offset is equal to A_1A_1''. It will not alter the current dynamic isotropy configuration and can be seen from Eqn. (1). As we move along $\boldsymbol{s_j}$ (say $\boldsymbol{\delta s_j}$ along the leg), the cross product, i.e., $({}^{\boldsymbol{P}}\boldsymbol{p_j}+\boldsymbol{\delta s_j})\times(\boldsymbol{s_j}) \approx {}^{\boldsymbol{P}}\boldsymbol{p_j}\times\boldsymbol{s_j}$ almost remains the same. This means we have the same [**B**] matrix and hence the same set of solutions. Moreover, incorporating active vibration control in a dynamically isotropic MGSP will improve the damping performance at peak along with better isolator performance in the isolation region. However, the cost and high-power requirement factor must be considered in active vibration isolation for spacecraft applications.

6 Conclusion

The research demonstrates the effectiveness of a dynamically isotropic Modified Gough Stewart platform (MGSP) for micro-vibration isolation. The study's findings, including the convergence of analytical, simulation, and experimental results, provide compelling support for this conclusion. Specifically, the first six natural frequencies and damping characteristics closely align with one another, thus validating the rationale for choosing a dynamically isotropic configuration for micro-vibration isolation purposes. Such a configuration ensures a well-defined isolation region within the micro-vibration frequency spectrum.

Acknowledgments

The authors wish to extend their gratitude to the scientists and personnel of the Indian Space Research Organization for their unwavering support during the experimentation process.

References

[1] Ahmad, N.: Vibration mitigation in spacecraft components using Stewart platform and particle impact damping. PhD Thesis, Indian Institute of Science (2020)

[2] Shyam, R.B.A., Ahmad, N., Ranganath, R., Ghosal, A.: Design of a dynamically isotropic stewart-gough platform for passive micro-vibration isolation in spacecraft using optimization. Journal of Spacecraft Technology **30**(2), 1–8 (2019)

[3] Preumont, A., Horodinca, M., Romanescu, I., de Marneffe, B., Avraam, M., Deraemaeker, A., Bossens, F., Abu Hanieh, A.: A six-axis single-stage active vibration isolator based on stewart platform. Journal of Sound and Vibration **300**(3), 644–661 (2007) https://doi.org/10.1016/j.jsv.2006.07.050

[4] Wang, C., Xie, X., Chen, Y., Zhang, Z.: Investigation on active vibration isolation of a stewart platform with piezoelectric actuators. Journal of Sound and Vibration **383**, 1–19 (2016) https://doi.org/10.1016/j.jsv.2016.07.021

[5] Hanieh, A.A.: Active isolation and damping of vibrations via Stewart platform. PhD Thesis, ULB ASL (2003)

[6] Singh, Y.P., Ghosal, A.: Dynamically isotropic gough-stewart platform design using a pair of triangles. In: Advances in Service and Industrial Robotics, pp. 264–272. Springer, Bled, Slovenia (2023). https://doi.org/10.1007/978-3-031-32606-6_31

[7] Singh, Y.P., Ahmad, N., Ghosal, A.: Design of dynamically isotropic modified gough- stewart platform using a geometry-based approach. In: Advances in Asian Mechanism and Machine Science, pp. 258–268. Springer, Hanoi, Vietnam (2021). https://doi.org/10.1007/978-3-030-91892-7_24

[8] Tong, Z., He, J., Jiang, H., Duan, G.: Optimal design of a class of generalized symmetric gough–stewart parallel manipulators with dynamic isotropy and singularity-free workspace. Robotica **30**(2), 305–314 (2011) https://doi.org/10.1017/s0263574711000531

[9] Jiang, H.-z., He, J.-f., Tong, Z.-z., Wang, W.: Dynamic isotropic design for modified gough–stewart platforms lying on a pair of circular hyperboloids. Mechanism and Machine Theory **46**(9), 1301–1315 (2011) https://doi.org/10.1016/j.mechmachtheory.2011.04.003

[10] Afzali-Far, B., Lidström, P.: A class of generalized gough-stewart platforms used for effectively obtaining dynamic isotropy – an analytical study. MATEC Web of Conferences **35**, 02002–15 (2015) https://doi.org/10.1051/matecconf/20153502002

[11] Yun, H., Liu, L., Li, Q., Li, W., Tang, L.: Development of an isotropic Stewart platform for telescope secondary mirror. Mechanical Systems and Signal Processing **127**, 328–344 (2019) https://doi.org/10.1016/j.ymssp.2019.03.001

[12] Yao, J., Hou, Y., Wang, H., Zhou, T., Zhao, Y.: Spatially isotropic configuration of stewart platform-based force sensor. Mechanism and Machine Theory **46**(2), 142–155 (2011) https://doi.org/10.1016/j.mechmachtheory.2010.10.002